Influence of complex impact of the picosecond electron beam and volume discharge in atmospheric-pressure air on the electronic properties of MCT epitaxial films surface

Denis V. Grigoryev*[a], Vadim A. Novikov[a], Dmitriy A. Bezrodnyy[a], Viktor F. Tarasenko[b], Michail A. Shulepov[b], Sergei A. Dvoretskii[c],
[a]Tomsk State University, 36 Lenin Av., Tomsk, 634050, Russia; [b]Institute of High Current Electronics SB RAS, 2/3 Akademichesky, Tomsk, 634055, Russia; [c]Institute of Semiconductor Physics SB RAS, Pr. Ac. Lavrentyeva, 13, Novosibirsk 630090, Russia

ABSTRACT

In the present report we studied the distribution of surface potential of the HgCdTe epitaxial films grown by molecular beam epitaxy after the impact of picosecond electron beam and volume discharge in atmospheric-pressure air. The surface potential distribution was studied by the Kelvin Force Probe Microscopy. The experimental data obtained for the variation of the contact potential difference (ΔCPD) between the V-defect and the main matrix of the epitaxial film. The investigation of the origin epitaxial films show that variation of the spatial distribution of surface potential in the V-defect region can be related to the variation of the material composition. The experimental data obtained for the irradiated samples show that the mean value of ΔCPD for the original surface differs from the one for the irradiated surface for 55 eV. At the same time the mean value of ΔCPD changes its sign indicating that the original surface of the epitaxial HgCdTe film predominantly contains the grains with increased cadmium content while after the irradiation the grains possess an increased content of mercury. Therefore, during the irradiation process a decrease of the mercury content in the near-surface region of the semiconductor takes place resulting in the alteration of the electrophysical properties in the films near-surface region.

Keywords: HgCdTe, epitaxial films, Kelvin Force Probe Microscopy, volume discharge

1. INTRODUCTION

Electric discharges of different types as well as electron beams are now widely used for the modification of near-surface layers of various materials[1]. It was reported that a high-voltage diffuse discharge at a low gas pressure and a low power could be used for the inactivation of microbiological cultures[2]. Also it was shown in[3, 4] that the metal surface can be modified and cleaned by a volume discharge induced by a runaway electrons preionized diffuse discharge (REP DD). At higher pressures of different gases, including air at atmospheric pressure, a volume (diffusion) discharge is formed in the inhomogeneous electrical field due to runaway electrons and X-ray radiation. A special feature of a REP DD is a possibility of realizing high specific power of energy contribution (up to 800 MW/cm^3)[5]. In so doing, beams of runaway electrons with the current amplitude of tens-to-hundreds amperes are generated from the discharge plasma, and the half-amplitude pulse duration of the beam current is in no excess of 100 ps[6]. Thus, during formation of a nanosecond volume discharge in the air, the anode is acted upon by a combination of a dense nanosecond-discharge plasma with the specific power of energy contribution of hundreds of megawatts per cubic centimeter and a supershort electron beam with a wide energy spectrum. In addition, the anode is affected by a shock wave as well as UV- and VUV radiation from the discharge plasma.

The ternary semiconductor compounds $Hg_{1-x}Cd_xTe$ (HgCdTe, MCT, x – material composition) are one of the major materials used for manufacturing the inherent infrared (IR) photodetectors for the wavelength ranges of 3-5 and 8-14 micrometers[7]. The heteroepitaxial MCT films grown by molecular beam epitaxy (MBE) are one of the most promising materials for manufacturing multi-element photodetecting devices capable of the signal processing directly in the focal region (FPA – focal plane array). Along with the study of the initial properties of epitaxial films of MCT grown by MBE a very urgent task is controlled changing of the parameters of the material in order to obtain the desired semiconductor structures. The investigations of the epitaxial growth process of MCT have shown that without reference to the substrate type there occurs the formation of macroscopic V-defects that represent the inclusions of polycrystalline phase of MCT with material composition different from that of the bulk of the epitaxial film[8, 9]. These defects are mostly impacted on

XII International Conference on Atomic and Molecular Pulsed Lasers, edited by Victor F. Tarasenko, Andrey M. Kabanov, Proc. of SPIE Vol. 9810, 98100S · © 2015 SPIE
CCC code: 0277-786X/15/$18 · doi: 10.1117/12.2224696

the performance capabilities of photosensitive element arrays in the focal plane. Because of the fact that the spectral range and sensitivity of the final photoelectric cell greatly depends on the material composition one of the important problems is not only to study but also to control the composition of both the individual crystal grains and the overall V-defect.

The aim of this work is to study the effect of picosecond electron beam and volume discharge in atmospheric-pressure air on the distribution of the surface potential in the V-defect regions of epitaxial MCT films.

2. EXPERIMENTAL APPARATUS AND METHODS

For experiments the samples of epitaxial $Hg_{1-x}Cd_xTe$ films of the n-type conductivity grown by MBE on GaAs (013) substrates with ZnTe and CdTe buffer layers were prepared at the Institute for Semiconductor Physics of the Siberian Branch of the Russian Academy of Sciences (Novosibirsk). The content of CdTe in the working layer of epitaxial films was x = 0.22. The width of the upper variband layer was close to 0.4 micrometers while the content of CdTe on the surface was 0.44. The value of the content x and the width of the epitaxial film were controlled by in situ ellipsometric measurements. The controlling of the content x was conducted based on the optical transmittance spectra at room temperature.

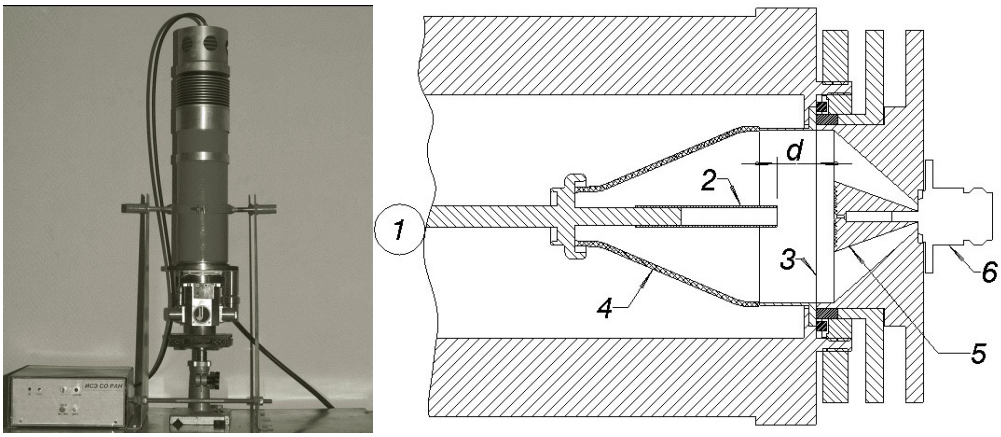

Figure 1. (a) - A setup with the discharge chamber and generator RADAN-220. (b) - Schematic diagram of the gas-filled diode and collector assembly: (1) connection to a high-voltage pulse generator; (2) cathode; (3) foil anode; (4) insulator; (5) cone-shaped collector; (6) connecting socket.

The irradiation of the MCT epifilms samples by REP DD was carried out on a specially designed setups. The image of setup is shown in figure 1a. The irradiations were performed using a discharge chamber, which is schematically depicted in figure 1b.The as-grown samples were placed in a gas diode on a copper anode. The samples were irradiated by 1200 pulses in the pulse-periodic mode at the pulse repetition rate of 1 Hz. A distance from a flat copper to a tubular electrode could be varied within 8–16 mm. The interelectrode voltage was supplied from a pulser of the RADAN-220 type, which generated voltage pulses with an amplitude of ~230 kV (in the open-circuit regime), a FWHM of ~ 2 ns (on a matched load), and a leading front width of ~ 0.5 ns. The discharge current was measured using a shunt composed of chip resistors connected between the foil anode and the discharge chamber housing. The results of measurements showed that the current pulse amplitude for both polarities of the applied voltage pulse was ~3 kA and the total duration of the discharge current pulse was ~30 ns (the first half-period of the discharge current pulse had a duration of ~8 ns). For the generator RADAN-220 that provided specific power input in gas discharge plasma above 0.8 GW/cm3 under atmospheric pressure of air, and electrodes spacing of 8 mm. The volumetric character of the discharge also remained at a pulse repetition rate of 3 kHz.

For the original surface and the one exposed to REP DD the surface potential distribution was studied by the Kelvin Force Probe Microscopy (KFPM). This method is widely used for studying the distribution of the inherent and surface potentials of instrumental micro-and nanostructures[10-12]. The measurements were performed on a commercial atomic-force microscope (AFM) "Solver HV" (produced by NT-MDT). We used polysilicon B-doped probes covered with platinum (probe type NSG11/Pt, manufactured by NT-MDT). To obtain the surface potential profile we measured the contact potential difference (CPD) distribution in between the AFM probe and the surface of the epitaxial film. The CPD

distribution was measured together with the surface morphology. In order to minimize the influence of the morphology on the CPD distribution we carried out our measurements at distance of sample-probe dz = 50-100 nm. The KPFM is a two-pass technique. In the first pass, one acquires the surface topography of a single line in Tapping Mode. Then by immediately retracing this topography over the same line at a set lift-height (typically, 50–100 nm)[13] from the sample surface one can measure the distribution of CPD. This procedure is then repeated for each line along the slow scan axis. In the second pass, DC and AC voltage are applied between the probe and the sample.

The electrostatic force interaction between the probe and the sample is given by

$$F_z = \frac{1}{2}\frac{dC}{dz}\left[U_{CPD}(\mathrm{x,y}) - \mathrm{U_{DC}} - U_{AC}\sin(\varpi\,\mathrm{t})\right]^2 \quad (1)$$

where $U_{CPD}(x, y)$ - local contact potential difference at coordinates x, y; U_{DC} - DC voltage applied between probe and sample; $U_{AC}\sin(\omega t)$ - AC voltage applied between probe and sample; dz - distance between tip of the probe and surface of sample; and C - capacitance between probe and sample. The KPFM measurements were performed at the ω component of F_z,

$$F_{\varpi} = \frac{dC}{dz}\left[U_{CPD}(\mathrm{x,y}) - \mathrm{U_{DC}}\right]U_{AC}\sin(\varpi\,\mathrm{t}) \quad (2)$$

As a result of the F_ω, the probe starts vibrating. If the U_{DC} applied to the probe is equal the $U_{CPD}(x, y)$, the force acting on the probe becomes zero. On other hand, the CPD can be written as

$$qU_{CPD}(x,y) = \varphi_{probe} - \varphi_{sample}, \quad (3)$$

where φ_{probe} and φ_{sample} - work functions of the probe and the sample, respectively; q - elementary electrical charge.

3. EXPERIMENTAL RESULTS AND DISCUSSION

Figure 2 demonstrates typical AFM images of the morphology of surface and distribution of surface potential of a V-defect of origin MCT epitaxial film. One can see that the value of surface potential of V-defect differs from that of the main material matrix. The measurements of the CPD were performed in at least 50 scanning fields of MCT epitaxial film. The average variation of the contact potential difference (ΔCPD) of V-defect with respect to the base material matrix of the epitaxial layer is about 50 mV and 80 mV. Thus, MCT epitaxial films have 2 typical average changes of the CPD value for V-defects. In order to eliminate the influence of the adsorption film on the measured value of CPD, we studied the CPD distribution in a vacuum (1×10^{-5} Torr). The study showed that the value of ΔCPD does not change and is within the error of measurement (10 mV). Some of the V-defects possess a non-uniform CPD distribution (Fig. 2) that is supposedly related to the variation of the solid solution composition of the crystal grains forming the defect.

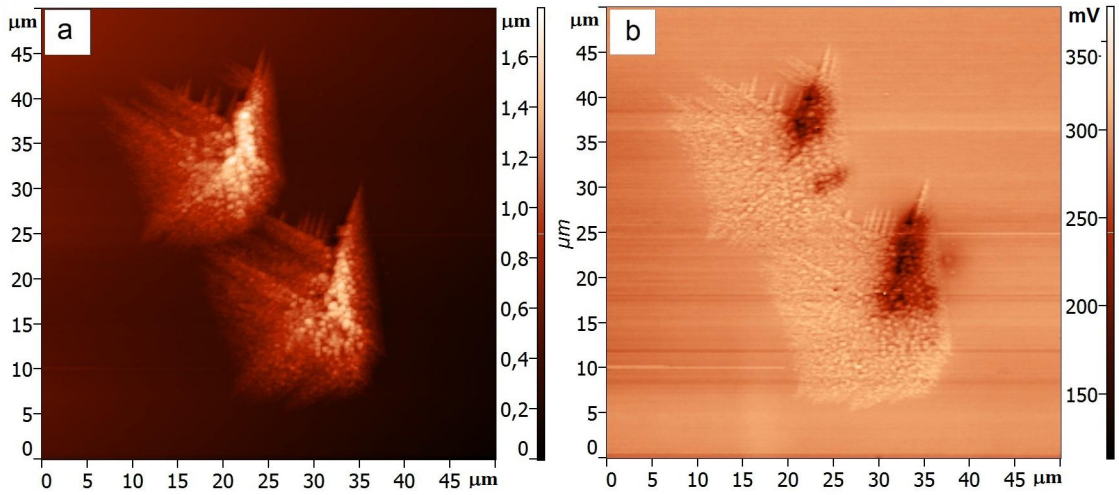

Figure 2 AFM image of morphology (a) and CPD (b) of the MCT epitaxial film in the vicinity of a V-defect.

The φ_{sample} (3) can have a component, which describes the band bending at the surface. If there is a band bending on the surface (in the absence of the pinning of the Fermi level at the surface), then φ_{sample} should depend on the electric field of probe, laser diffraction of optical system of AFM and composition (x) of the solution of $Hg_{1-x}Cd_xTe$. In our study, we changed the voltage of the probe, so that the potential of the probe varied from −7 V to +7 V and the U_{AC} varied from 1 V to 8 V. The ΔCPD did not change. This means that if there is a band bending on the surface, the ΔCPD does not depend on the potential of the probe. The field of laser diffraction is moved in accordance with the probe position. So that if the band bending changes the energy of laser diffraction, then this change is constant for the entire region of observation and does not lead to a change of ΔCPD. Thus, the change of ΔCPD depends on the composition of the solution of MCT. Since the variation of the MCT solid solution composition is insignificant one can disregard the induced by it variation of the band bending on the surface.

It follows from the above that the value of the CPD is defined by the work function of the probe and the sample. Since the work function of the solid solution is determined by the $Hg_{1-x}Cd_xTe$ epitaxial film composition (x), the variation of the CPD spatial distribution can be associated with the variation of the MCT solid solution composition.

The variation of the solid solution composition of a V-defect can be estimated if one takes into account that the CPD value is equal to the difference of work functions of the AFM probe and the surface of the sample[14]. The AFM probe work function remains constant during the measurement process. Using a linear approximation for the $Hg_{1-x}Cd_xTe$ solid solution work function (the work functions of CdTe and HgTe equal to 4.5 eV and 5.9 eV, respectively[15]), the definition for the CPD variation in a V-defect can be written in the following form:

$$\Delta CPD = \varphi_2 - \varphi_1, \tag{4}$$

$$\varphi_i = x_i\varphi_{CdTe} - (1 - x_i)\varphi_{HgTe}, \tag{5}$$

where φ_i is the work function of the MCT solid solution with a given composition. Then the variation of the solid solution composition can be expressed through $Hg_{1-x}Cd_xTe$ as

$$dx = x_2 - x_1 = \frac{\Delta CPD}{\varphi_{CdTe} - \varphi_{HgTe}}, \tag{6}$$

Taking into account that for a V-defect ΔCPD = 50 mV, it can be seen from (6) that the mercury content in the solid solution composition should increase for 0.036, for ΔCPD = 80 mV, dx = 0.057.

A typical image of the distribution of the CPD for irradiated samples by REP DD is presented on figure 3. One can see that the distribution is significantly inhomogeneous, exhibiting regions where the CPD is either lower or higher than that of the epitaxial film. On the periphery of each individual crystal grain there is a dramatic variation of the CPD, which can indicate the presence of a modified potential.

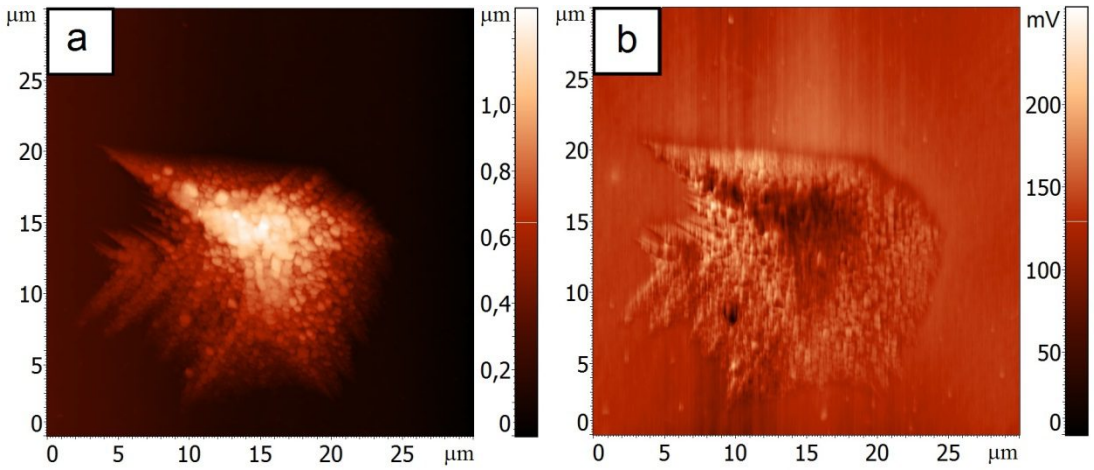

Figure 3 AFM image of a V-defect surface morphology (a) and the distribution of the surface potential or CPD (b).

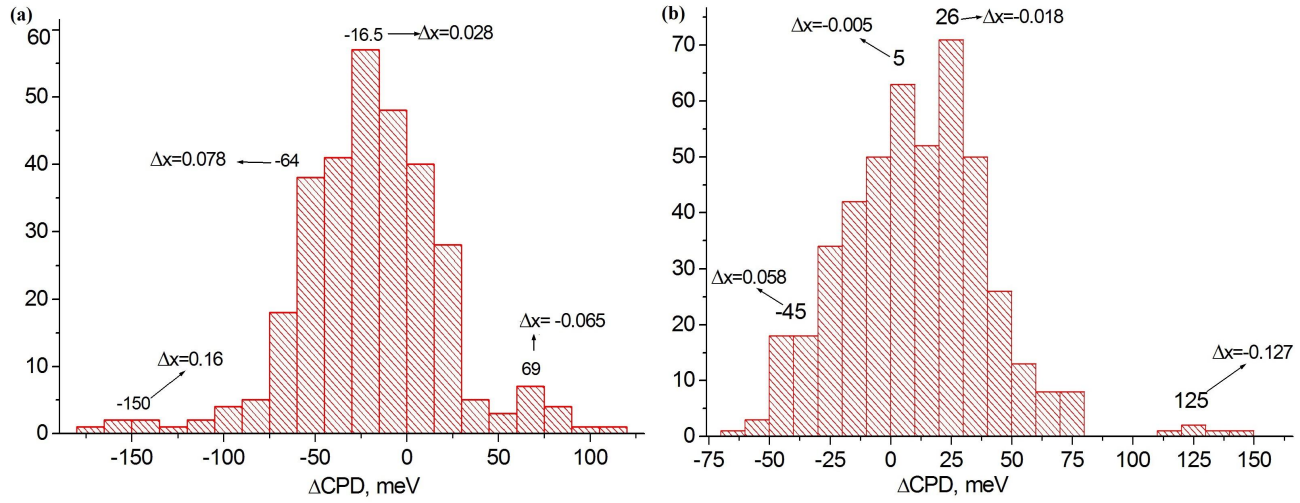

Figure 4 Distribution of the deviation of the CPD value of individual crystal grains of a V-defect versus the CPD of the epitaxial film: a) original film; b) after irradiation, 1 – distribution of ΔCPD, 2 – assemblage of normal distributions, 3 – combined distribution; the arrows indicate the variation Δx of the CdTe content for the given value of ΔCPD.

Using the distribution of the surface potential we derived the difference (ΔCPD) between the CPD value for individual crystal grains of a V-defect and the mean value of the CPD of epitaxial film. The distributions of the ΔCPD for a film before and after exposure to radiation are presented on figure 4. The ΔCPD distribution possesses a complex character and can be described by an assemblage of normal distributions. Since the work function of the cantilever needle-point does not change during the measurement process it becomes clear that the observed changes are related to the local changes of the MCT work function, i.e. the changes of the work functions of individual crystal grains of the V-defect are observed. Using the expression for the dependency of the $Hg_{1-x}Cd_xTe$ solid solution electron affinity on the component composition[16] one can write the expression for the ΔCPD in the following form:

$$\Delta CPD = \left[1.29 - 7.13 \cdot 10^{-4} T\right]\left(x_1 - x_2\right) - 0.54\left(x_1^2 - x_2^2\right) + 0.56\left(x_1^3 - x_2^3\right) \qquad (7)$$

where x_1 is the cadmium content in the epitaxial film and x_2 is the cadmium content in a selected V-defect crystal grain. It is fair to assume that the value of x_1 does not change, in that case one can use the value of the ΔCPD to derive the value of Δx that characterizes the variation of the cadmium content in a selected crystal grain relative to the epitaxial film.

Taking into account the expression (7) and the data presented on the figure 3 one can show that before and after the exposure to radiation individual crystal grains of a V-defect may possess a higher mercury content ($\Delta x < 0$) as well as a higher cadmium content ($\Delta x > 0$). In the original unirradiated sample the crystal grains with a higher mercury content prevail while in the irradiated sample dominate the grains with a higher cadmium content. Given the complex character of the ΔCPD distribution consider the mean values of this parameter for the original (27 mV) and the irradiated (-28 mV) surface of MCT. These mean values differ for 55 eV. Note also that the mean value of the ΔCPD changes its sign. Using the expression (7) it can be shown that the original surface of the HgCdTe epitaxial film mainly contained the crystal grains with an increased mercury content while the irradiated surface mainly contains the crystal grains with an increased cadmium content. It follows that during the irradiation process the decrease of the mercury content in the semiconductor near-surface region takes place and, hence, occur the changes of the electrophysical properties in the near-surface region of the film.

4. CONCLUSION

In conclusion, the present paper deals with the surface potential distribution of MCT epitaxial films grown by MBE before and after impact of a picosecond electron beam and volume discharge in atmospheric-pressure air. The experimental data for the origin epitaxial film was shown that that variation of the spatial distribution of surface potential in the V-defect region can be related to the variation of the material composition. The experimental data obtained for the irradiated samples show that the exposure to the radiation of nanosecond volume discharge leads to changes of the

material composition of the solid solution of individual V-defect crystal grains. As the decrease of the mercury content is expected to be observed not only in the crystal grains but also in the overall epitaxial film, one can infer that the mercury desorption rate is higher for the crystal grains than for the film itself.

This research was supported by grant (№14-29-00052) from Russian Science Foundation.

REFERENCES

[1] Didenko, A. N., Sharkeev, Yu. P., Kozlov, E. V., et al. [Long-Range Effects in Ion-Implanted Metallic Materials], Izd. Nauchn. Techn. Literarury, Tomsk (2004).
[2] Buranov, S.N., Voevodin, S.V., Voevodina, I.A., et. al. "The effect of a high-voltage diffuse gas discharge on microbiological cultures," High Temp. 43, 361-367 (2005).
[3] Shulepov, M.A., Akhmadeev, Y.K., Tarasenko, V.F., et. al. "Modification of surface layers of copper under the action of the volumetric discharge initiated by an avalanche electron beam in nitrogen and CO2 at atmospheric pressure," Russian Physics Journal 53, 1290-1294 (2011).
[4] Shulepov, M.A., Tarasenko, V.F., Goncharenko, I.M., et. al. "Modification of the near-surface layers of a copper foil under the action of a volume gas discharge in air at atmospheric pressure," Technical Physics Letters 34, 296-299 (2008).
[5] Alekseev, S.B., Gubanov, V.P., Kostyrya, I.D., et. al. "Pulsed volume discharge in a nonuniform electric field at a high pressure and the short leading edge of a voltage pulse," Quantum Electronics 34, 1007-1010 (2004).
[6] Tarasenko, V.F. "Parameters of a supershort avalanche electron beam generated in atmospheric-pressure air," Plasma Physics Reports 37, 409-421 (2001).
[7] Rogalski, A. [Infrared Detectors], CRC Press, Boca Raton (2011).
[8] Sidorov, Yu. G., Dvoretskii, S. A., Varavin, V. S., Mikhailov, N. N., Yakushev, M. V.,Sabinina, I. V. "Molecular-beam epitaxy of mercury-cadmium-telluride solid solutions on alternative substrates," Semiconductors 35, 1045-1053 (2001).
[9] Sabinina, I. V., Gutakovsky, A. K., Sidorov, Yu. G., Latyshev, A. V. "Nature of V-shaped defects in HgCdTe epilayers grown by molecular beam epitaxy," Journal of Crystal Growth 274, 339-346 (2005).
[10] Chun-Sheng, J., Moutinho, H. R., Friedman, D. J., Geisz, J. F., Al-Jassim, M. M. "Measurement of built-in electrical potential in III-V solar cells by scanning Kelvin probe microscopy," Journal of Applied Physics 93, 10035-10040 (2003).
[11] Cai, L. X., Wang, H. M. "Microstructure and dry-sliding wear resistance of laser clad tungsten reinforced W5Si3/W2Ni3Si intermetallic coatings," Applied Surface Science 235, 501-506 (2004).
[12] Katzer, Kl. D., Mertin, W., Bacher, G., Jaeger, A., Streubel, K. "Voltage drop in an (AlxGa1-x)0.5in 0.5P light-emitting diode probed by Kelvin probe force microscopy," Applied Physics Letters 89, 103522 (2006).
[13] Vatel, O., Tanimoto M. "Kelvin probe force microscopy for potential distribution measurement of semiconductor devices," J. Appl. Phys. 77, 2358 (1995).
[14] Torkhov, N. A., Novikov, V. A. "Fractal geometry of the surface potential in electrochemically deposited platinum and palladium films," Semiconductors 43, 1071 (2009).
[15] Zozime, A., Vermeulin, C. "Properties of sputtered mercury telluride contacts on p-type cadmium telluride," Rev. Phys. Appl. 23, 1825 (1988).
[16] Voitsekhovskii, A. V., Gorn, D. I., Izhnin, I. I., et. al. "Analysis of the photoluminescence spectra of CdxHg1-xte heteroepitaxial structures with potential and quantum wells grown by molecularbeam epitaxy," Russian Physics Journal 55, 910-916 (2013).